Study of resistive MHD stability of COMPASS Upgrade scenarios

A. Casolari[1], L. Pigatto[2], O. Bogar[1], M. Farnik[1], M. Imrisek[1], F. Jaulmes[1],
L. Kripner[1], Y.Q. Liu[3], T. Markovic[1], M. Peterka[1], V. Yanovskiy[1]

[1] *Institute of Plasma Physics of the CAS, Prague, Czech Republic*

[2] *Consorzio RFX and CNR-ISTP, Padova, Italy*

[3] *General Atomics, San Diego, Unites States of America*

The planned operational scenarios for COMPASS Upgrade will explore a broad range of parameters, such as magnetic field ($2.5 \leq B \leq 5$ T) and plasma current ($0.8 \leq Ip \leq 1.6$ MA) [1]. These scenarios, which represent the baseline for COMPASS-U operation, are labeled as early H-mode, ITER-like H-mode and high-performance H-mode. Other two scenarios that deviate from the baseline, either due to a larger plasma current or the shape of the plasma, have been explored; they are labeled as high-current and negative-triangularity.

Name	Scenario	$B[T]$	$I_P[MA]$	q_{95}	β_N
Early H-mode	3210	2.5	0.8	3.6	1.52
ITER-like H-mode	24300	4.3	1.3	3.8	1.19
High-perf. H-mode	5400	5.0	1.6	3.4	1.15
High-current	4320	4.3	1.8	2.7	0.96
Negative-triang.	11200	1.26	0.3	2.8	1.90

Study of linear stability of COMPASS-U scenarios was performed with the MARS-F code [2], in the single-fluid framework. Systematic parametric scans were made to determine the operational limits of the different scenarios and to identify the most unstable MHD modes [3]. All the scenarios we explored are characterized by $q_{min} < 1$, which makes them potentially unstable to internal kink mode. The safety factor profile q was artificially modified with the equilibrium code CHEASE so that $q_{min} > 1$, while keeping the global q profile, the current and pressure profiles mostly unchanged. β_N for all scenarios falls below the no-wall limit β_{NW}, which means that the scenarios are ideally stable with respect to external kink modes.

Linear tearing mode

Stability with respect to TMs was addressed by performing resistivity scans. The scaling of the growth rate with $S^{-3/5}$ was recovered in most of scenarios, with small deviations. A scan over β was performed to evaluate the stabilizing Glasser–Greene–Johnson (GGJ) effect. In the baseline scenarios, the results show that the growth rate drops to zero as β_N reaches the nominal value, and the mode develops a finite rotation frequency. In scenario #5400, in the low S limit

(high resistivity), the growth rate does not drop to zero as β_N reaches the nominal value, but it reaches a minimum for some intermediate β_N and then it grows again.

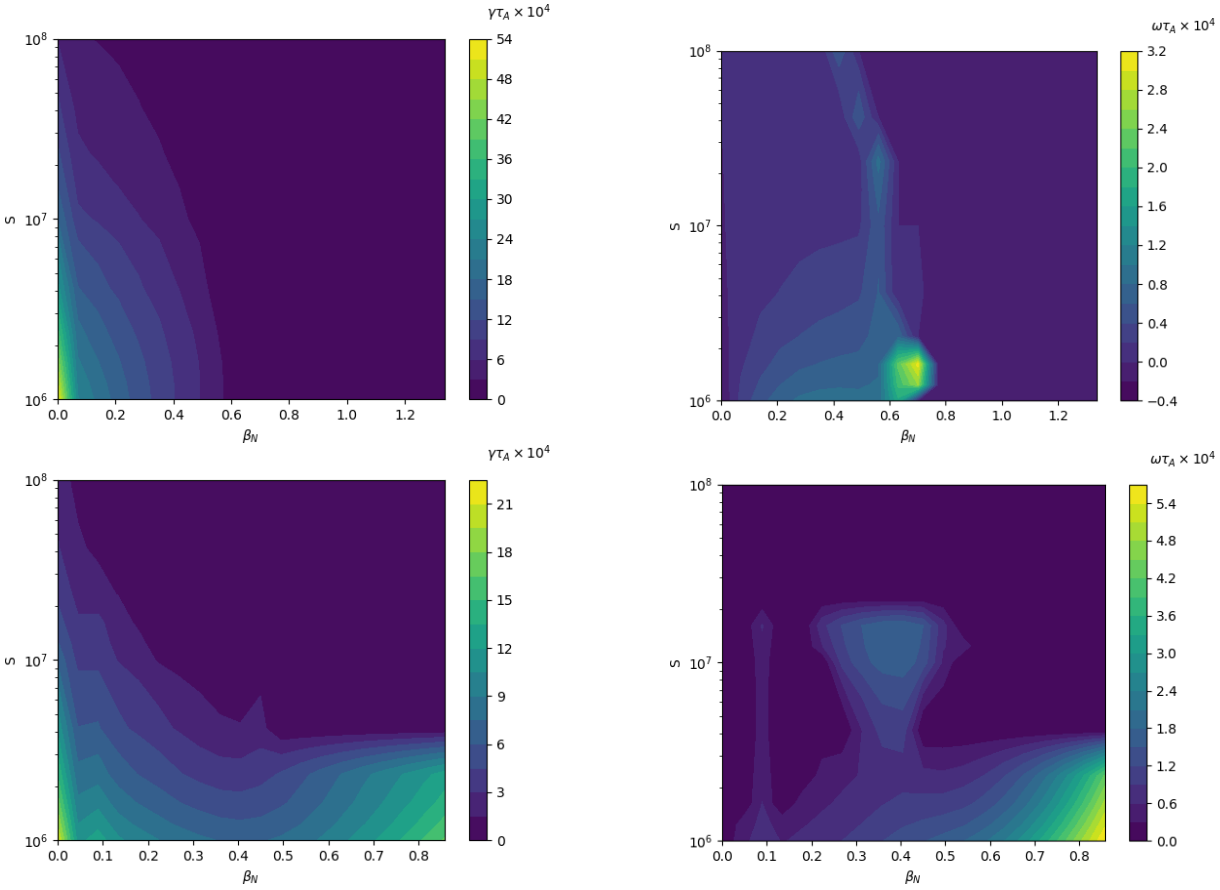

Figure 1: Growth rate (left) and frequency (right) normalized to Alfven time as function of S and β_N for #3210 (top) and #5400 (bottom)

The introduction of an ideal wall positioned at $r/a = 1.1$ produced complete stabilization for nominal β_N, even in the low-S limit. We conclude that the stabilization at intermediate β_N can be attributed to GGJ while mode destabilization taking place at larger β_N is to be attributed to the coupling with external modes. In COMPASS-U tokamak the wall is relatively far from the plasma ($r/a \approx 1.5$), thus its stabilizing effect on the external modes is negligible. The high-current and negative-triangularity scenarios are characterized by lower q_{95}, which means that the $q = 2$ rational surface is closer to the plasma edge and leads to different stability properties. When finite β is included in the calculations, the behavior is significantly different from the previous set of scenarios. Here we observe that the growth rate slightly drops but then it grows to even larger values for nominal β. When an ideal wall is introduced close to the plasma surface, a significant stabilization is achieved.

TMs located near the plasma edge (associated with low q_{95}) were found to be more unstable in NT plasma because of the lack of favorable curvature stabilization. However, the same finite-β destabilization takes place in the high-current scenario, which possesses a similar q-profile. This suggests that the mechanism of destabilization in our case should be traced back to a coupling with external, pressure-driven modes. The presence of an unreconnected $q = 3$ surface shields the (2,1) TM from the destabilizing influence of the (3,1) external kink mode [4], thus the finite-β destabilization of the (2,1) TM in the low q_{95} scenarios must be attributed to coupling with the (3,1) external kink mode.

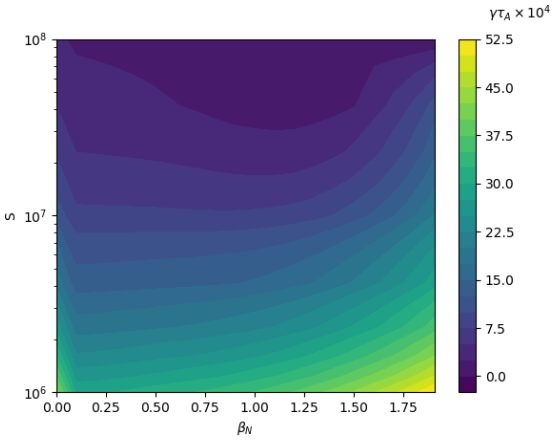

Figure 2: Growth rate normalized to Alfven time as function of S and β_N for #11200

Neoclassical tearing modes

Magnetic islands are the result of the nonlinear evolution of TMs. When neoclassical effects are kept into account, the perturbed bootstrap current can drive the mode unstable even if $\Delta' < 0$: in this event, the mode is named 'neoclassical tearing mode', or NTM [5]. Dynamics of NTMs is described by the generalized Rutherford equation (GRE):

$$\frac{\tau_R}{r_s^2}\frac{dW}{dt} = \Delta' + \Delta'_{BS} + \Delta'_{GGJ} + \Delta'_{pol} + \Delta'_H + \Delta'_{CD} \tag{1}$$

where τ_R is the resistive time of the plasma, r_s is the radius of the rational surface, w is the island width, Δ' is the linear stability index corrected for the island saturation, Δ'_{BS} is the contribution from bootstrap current, Δ'_{GGJ} is the stabilizing GGJ effect, Δ'_{pol} is the contribution from polarization current, Δ'_H and Δ'_{CD} are the contributions from electron cyclotron heating (ECH) and current drive (ECCD). The saturation width w_s for the NTMs in the considered scenarios is comparable to the distance between the $q = 2$ surface and the edge of the plasma, which make them susceptible to locking to error fields. ECH and ECCD are the most widely adopted strategies to control and suppress NTMs. To realize the NTM suppression by EC waves, a poloidal and toroidal steering of the EC beam is necessary to aim precisely at the rational surface; this requires the design of a launcher equipped with steering mirrors. In the scenarios we considered, for 1 MW of EC power the EC driven current is smaller than the bootstrap current by at least one order of magnitude.

For island width larger than the deposition width of EC ($w/w_{dep} > 1$), ECH proves to be more efficient than ECCD in stabilizing NTMs [6]. The calculation of ECH and ECCD conversion efficiencies proves that ECH provides a sufficient stabilizing effect with only 2 MW of EC power. Efficiencies of ECCD and ECH are very sensitive to the misalignment between the EC power deposition and the position of the rational surfaces: the radio frequency (RF) current condensation effect [7] can help reduce both the minimum required power and the accuracy in EC beam injection.

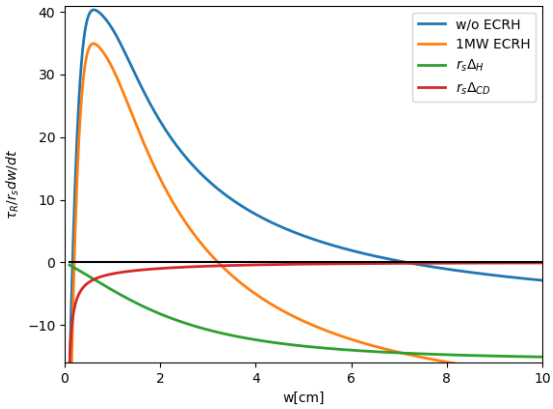

Figure 3: Right-hand side of GRE together with the contributions from heating (Δ'_H) and current drive (Δ'_{CD})

Conclusions

The baseline scenarios, characterized by $3 < q_{95} < 4$, are expected to be stable with respect to TMs at nominal β because of the stabilizing GGJ effect. The negative-triangularity and high-current scenarios are characterized by $q_{95} < 3$ and present a significant component of external kink modes in the spectrum, which make them unstable for nominal β even for realistic plasma resistivities. EC heating is expected to be significantly more efficient than CD at stabilizing NTMs in our scenarios: this will have consequences on the design of dedicated wave launcher. Preliminary evaluation of the current condensation in the examined scenarios suggests that its effect is expected to be small for the EC powers envisaged for the initial phase of operation.

Aknowledgements

The authors would like to thank E. Poli, N. Bertelli, N. J. Fisch and A. H. Reiman for the useful discussions. This work has been carried out within the framework of the project COMPASS-U: Tokamak for cutting-edge fusion research (No. *CZ*.02.1.01/0.0/0.0/16_019/0000768) and co-funded from European structural and investment funds and by MEYS project LM2023045.

References

[1] M. Komm et al., Nuclear Fusion **64**, 076028 (2024)

[2] Y. Liu et al., Phys. Plasmas **7**, 3681 (2000)

[3] A. Casolari et al., Plasma Phys. Control. Fusion **68** 025006 (2026)

[4] R. Fitzpatrick et al., Nucl. Fusion **33**, 1533 (1993)

[5] O. Sauter et al., Plasma Phys. Control. Fusion **44**, 1999 (2002)

[6] D. De Lazzari D & E. Westerhof, Nucl. Fusion **49**, 075002 (2009)

[7] A. Reiman & N. Fisch, Phys. Rev. Lett. **121**, 225001 (2018)